



Altitude cascade control of an avian-like flapping robot considering articulated wings and quasi-steady

S. Leyci, J. Poshtan*

Department of Electrical Engineering, Iran University of Science and Technology, Tehran, Iran

ABSTRACT: This paper intends to stabilize the flight of an avian-scale flapping robot with articulated. Modeling has been performed using Multibody dynamics, considering a tail. The equations of motion have been derived from Lagrange equations. Kampf mechanism, inspired by the birds, is used to drive the inner and outer wings with a phase shift. The aerodynamic model has been obtained from applying the blade element theory to the wings divided into twelve elements, considering the inner and outer wing distinction. The aerodynamic forces emerging from the movement of wing elements, in terms of flapping frequency and flight speed, are determined separately. Regarding the flight path angle and effective angle of attack, aerodynamic forces of the entire wings have been achieved in horizontal and vertical axes. The coupling of aerodynamic and dynamic completes the nonlinear time-periodic equations. Due to the impact of the fuselage pitch angle on the flight altitude, the cascade control was used to control fuselage and tail pitch angles in inner loops and altitude in the outer one. Proportional-derivative-integral control has been used to control the performance of the loops, the coefficients of which have been optimally designed

Review History:

Received: Feb. 16, 2020
Revised: Jul. 01, 2020
Accepted: Aug. 18, 2020
Available Online: Dec. 15, 2020

Keywords:

Flapping flight
Articulated wings
Cascade control
Altitude control
Quasi-steady aerodynamic

1- Introduction

By considering the degrees of freedom for the tail of the robot, it is possible to control the degrees of freedom of the body (thus changing the direction and navigation of the robot would be possible) in constant flight speed. The presence of a tail has several advantages, for example, improvements in static stability, simpler control strategies, and separation of wing and tail control units. However, tail aerodynamics is very complex due to the interference of wing and tail flows and is generally not considered in the modeling. The combination of the tail and articulated wings leads to an optimal performance with a simpler design. Tail improves forward flight performance, and static and dynamic stability, as well [1].

After obtaining the complete correspondence aerodynamic forces with the kinematics and dynamics of the ornithopter, the cascade control is used. Attitude control is in the low-level control category. In practice, due to limitations in structure, weight, and processing speed, the simplest control methods are proposed. In this study, cascade control is appropriate and satisfies the intent of the research. In this method, problems caused by nonlinear dynamics and vibrations, are solved in the inner loop. Finally, easier and faster control is achieved.

2- Dynamic Modeling

This system consists of a set of rigid objects connected in a tree structure. There are local fixed frames for each part. The equations of motion have been described in

the generalized coordinates. The Lagrange equation is obtained from $L = T - U$, where T , and U are kinetic and potential energies, respectively. Final equations of motion are achieved by placing the Lagrangian in Eq. (1).

$$\frac{d}{dt} \left(\frac{\partial L}{\partial \dot{q}} \right) - \frac{\partial L}{\partial q} + \frac{\partial C}{\partial \dot{q}} + \left[\frac{\partial \psi}{\partial q} \right]^T \lambda = Q \quad (1)$$

Here C is a function of energy loss, ψ is an algebraic constraint, and λ is the Lagrangian coefficient for the constraints. The constraint function is assumed to be zero [2]. The kinetic energy is obtained from the Eq. (2) where $M(q)$ is the mass matrix.

$$T = \frac{1}{2} \dot{q}^T M(q) \dot{q} \quad (2)$$

Assuming that the mass of the body is centered, the potential energy of the robot with n links is equivalent to:

If the robot has elasticity, then the potential energy will also include the energy stored in the elastic components [3]. After simplification, the equations of motion are

$$U = \sum_{k=1}^n U_k = \sum_{k=1}^n m_k g^T r_{ck} \quad (3)$$

*Corresponding author's email: jposhtan@iust.ac.ir



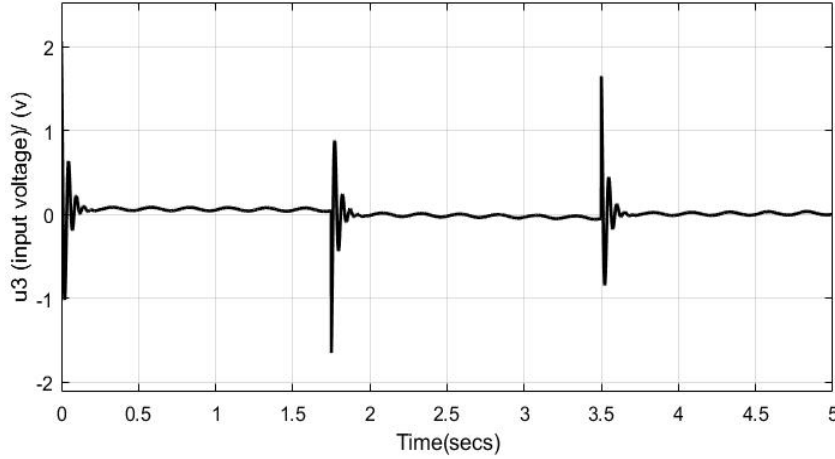


Fig. 1. The control signal for the third control loop

$$M(q)\ddot{q} + C(q, \dot{q})\dot{q} + Kq + g_k + N(q) = Q(q) \quad (4)$$

where k and g_k are the generalized stiffness matrix and the generalized gravity force, respectively. For simplicity, the stiffness matrix is set to zero [4]

3- Aerodynamic Model

Each wing divided into twelve sections with similar orientations, preserving the border of the inner and the outer wing [4]. The position of each section in the wing root frame is achieved considering the plunging and twisting.

The total drag force is the summation of the induced and parasite drag forces. Elliptic reduction factor, e , is also considered.

$$D_{total} = D_i + D_p = \frac{2(W \cos \gamma)^2}{e\pi B^2 \rho U_{ref}^2} + \frac{\rho U_{ref}^2 S_w C_f K}{2} \quad (5)$$

From the thin airfoil theory, the lift coefficient is given in Eq. (20).

$$C_l = 2\pi \sin(\alpha_{eff}) \quad (6)$$

These equations are applied to each section with a specific orientation and motion. Eq. (7) gives the circulatory lift coefficient, where d_c is the local chord length.

$$C_{l_c} = 2\pi C(k) \sin \alpha_{rel} + 0.636\sqrt{l/d_c} \quad (7)$$

This lift coefficient can be converted to the lift force for an element with a length of d_c and a width of d_r . The

circulatory lift is perpendicular to the flow rate and creates vertical and horizontal forces:

$$dN_{nc} = -\frac{\rho\pi(d_c^2)}{4}(\dot{\theta}U + \dots + r\ddot{\beta} \cos \theta - ba\ddot{\theta}).d_r \quad (8)$$

Since the local orientation varies over the wingspan, the vertical and horizontal forces must be computed before summing them up [2].

$$F_{vert} = \left[\sum_{n=1}^{12} dF_{vert_c} + dF_{vert_{nc}} \right] + D \sin \phi \cos(\gamma + \delta)$$

$$F_{horiz} = \left[\sum_{n=1}^{12} dF_{horiz_c} + dF_{horiz_{nc}} \right] + D \cos \phi \cos(\gamma + \delta) \quad (9)$$

4- Altitude Control

Cascade control is a control algorithm consisted of loops in which the output of one control loop determines the target of the next one. The robot's fuselage pitch angle will be used to control the flight altitude. Increasing the pitch angle to a certain range that does not lead to the dynamic stall, will increase the altitude. Therefore, the first controlling loop is created: The reference signal is the height rate, and the output is the reference fuselage pitch angle as an input to the second loop. The second loop is for the fuselage pitch control.

The third controller delivers the tail pitch to the desired reference point. The output of this controller determines the amount of voltage needed to bring it to the referenced value. Proportional-Integral-Derivative (PID) controllers are used to design the controllers.

$$C(s) = k_p + k_D s + \frac{K_I}{s} \quad (10)$$

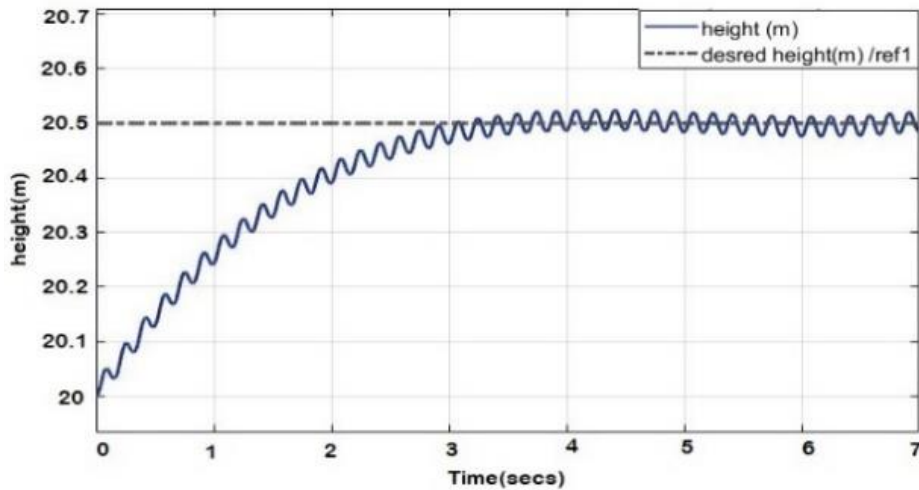


Fig. 2. Robot height control using a cascade control algorithm

5- Results

The control design of cascade loops starts from the most inner one. Fig. 1 shows the u_3 control signal, which is the input voltage to the tail actuator to create the torque needed to change the position of the tail and track the reference input. This signal is within the range of the applied voltage to the actuator. Finally, the robot can fly steadily at any altitude (Fig. 2).

6- Conclusions

In this paper, the performance of an avian-like flapping robot with articulated wings is investigated. Nonlinear time-periodic modeling is completed by appending the aerodynamic forces with the dynamics. Cascade control is implemented to control the flight altitude. Since the inner loop was faster than the outer one, the control speed was satisfying. It was safe to adjust the altitude at almost a constant flight speed.

References

- [1] S. Armanini, J. Caetano, C. De Visser, M. Pavel, G. De Croon, M. Mulder, Modelling wing wake and tail aerodynamics of a flapping-wing micro aerial vehicle, *International Journal of Micro Air Vehicles*, 11 (2019) 1756829319833674.
- [2] J.V. Caetano, C. De Visser, G. De Croon, B. Remes, C. De Wagter, J. Verboom, M. Mulder, Linear aerodynamic model identification of a flapping wing mav based on flight test data, *International Journal of Micro Air Vehicles*, 5(4) (2013) 273-286.
- [3] D. Tang, H. Zhu, W. Yuan, Z. Fan, M. Lei, Measuring the flexibility matrix of an eagle's flight feather and a method to estimate the stiffness distribution, *Chinese Physics B*, 28(7) (2019) 074703.
- [4] C. Altenbuchner, J.E. Hubbard Jr, *Modern Flexible Multi-Body Dynamics Modeling Methodology for Flapping Wing Vehicles*, Academic Press, 2017.

HOW TO CITE THIS ARTICLE

S. Leyci, J. Poshtan, *Altitude cascade control of an avian-like flapping robot considering articulated wings and quasi-steady*, *Amirkabir J. Mech. Eng.*, 53(4) (2021) 511-514.

DOI: [10.22060/mej.2020.17937.6691](https://doi.org/10.22060/mej.2020.17937.6691)



